processes

MDPI

Article

Fast Assisted History Matching of Fractured Vertical Well in Coalbed Methane Reservoirs Using the Bayesian Adaptive Direct Searching Algorithm

Zhijun Li

Exploration and Development Research Institute, PetroChina Huabei Oilfield Company, Cangzhou 062552, China; hzb_lzj@petrochina.com.cn

Abstract: The proper understanding of reservoir properties is an important step prior to forecasting fluid productions and deploying development strategies of a coalbed methane (CBM) reservoir. The assisted history matching (AHM) technique is a powerful technique that can derive reservoir properties based on production data, which however is usually rather time-consuming because hundreds or even thousands of numerical simulation runs are required before reasonable results can be obtained. This paper proposed the use of a newly developed algorithm, namely the Bayesian adaptive direct searching (BADS) algorithm, for assisting history matching of fractured vertical CBM wells to derive reservoir property values. The proposed method was applied on representative fractured vertical wells in the low-permeable CBM reservoirs in the Qinshui Basin, China. Results showed that the proposed method is capable of deriving reasonable estimates of key reservoir properties within a number of 50 numerical simulation runs, which is far more efficient than existing methods. The superiority of the BADS algorithm in terms of matching accuracy and robustness was highlighted by comparing with two commonly used algorithms, namely particle swarm optimization (PSO) and CMA-ES. The proposed method is a perspective in laboring manual efforts and accelerating the matching process while ensuring reasonable interpretation results.

Keywords: coalbed methane; assisted history matching; numerical simulation; Bayesian adaptive direct searching (BADS); fractured vertical well

Citation: Li, Z. Fast Assisted History Matching of Fractured Vertical Well in Coalbed Methane Reservoirs Using the Bayesian Adaptive Direct Searching Algorithm. *Processes* **2023**, *11*, 2239. https://doi.org/10.3390/pr11082239

Academic Editors: Zheng Sun, Tao Zhang, Dong Feng, Wen Zhao and Hung Vo Thanh

Received: 14 May 2023
Revised: 8 July 2023
Accepted: 10 July 2023
Published: 26 July 2023

1. Introduction

Coalbed methane (CBM) has been considered to be a hazardous gas for underground coal mining activities that may potentially lead to serious disasters such as coal and/or gas outburst and gas explosion [1,2]. The development and utilization of the CBM gas is beneficial to improving underground mining safety, reduction of gas emission into the atmosphere and adding to world's energy supply [3]. To date, commercial development of CBM has been active in the countries such as the United States, China, Australia, India and Indonesia [4,5]. Although complex completion techniques such as multi-fractured horizontal well, multi-lateral horizontal and cavity have been proposed to accelerate CBM production, the hydraulic stimulated vertical wells are still the most viable option for economic development of low-permeability CBM reservoirs.

Prior to the commercial extraction of a CBM reservoir, key formation properties exerting profound effect of well productions should be reasonably estimated in order to evaluate the economic feasibility and to deploy proper development strategies (e.g., optimization of well type, placement and drainage schedule). Basically, laboratory measurements are one of the important first steps for estimating the values of the reservoir properties [6]. However, the experimental result may not fully represent the reservoir-scale characteristics due to the strong heterogeneity nature of coal seams scale. Moreover, coal samples used for laboratory experiments are typically retrieved using certain coring techniques (e.g., wireline coring and pressure coring) [7,8] that are quite expensive, and thus the experimental data are

usually available only for a very limited number of evaluation wells. Compared with the laboratory experiment method, history matching of well production data is considered to be the most economic method that gains in-depth understanding of the reservoir behavior and gives estimation of reservoir parameters exerting critical effects on well productions. A successful history match gives confidence about the estimated reservoir parameters and their distribution during production and may indicate how the reservoir may behave under different reservoir management conditions. The history matching method has been extensively used to estimate coal seam properties. Karacan [6] integrated the single-well production history matching with geostatistical proxy model to estimate the dynamic properties including gas content, gas saturation and pressure in the Black Creek coal seam of Black Warrior Basin. Feng et al. [9], Zhou [10] and Zhang et al. [11] demonstrated the use of history matching to evaluate the formation properties based on production data from vertical fractured, casing horizontal and multi-fractured horizontal wells, respectively.

Although history matching is an important and perhaps the most reliable method to estimate the formation properties, it can be quite challenging due to the large number of properties with strong uncertainties properties that lead to a wide range of reservoir responses [12]. The impacts of coalbed parameters on methane production were extensively investigated [13–15]. It was reported that coalbed parameters with the greatest impact on simulation forecasts were adsorbed gas content, desorption isotherm, water saturation, coalbed thickness, permeability, porosity, compressibility and relative permeability. These parameters may exhibit strong variations both across the plane and the layers [11]. Thus, history matching is usually quite time-consuming because a number of trials of numerical simulations may be needed before successful matching is obtained.

The assisted history matching (AHM) method has been proposed and successfully applied for estimating oil and/or gas reservoir properties [16]. The AHM method in the petroleum engineering field was first proposed for conventional sandstone reservoirs to deduce the formation properties that are difficult to measure directly from field-scale historical production data [17]. During the past two decades, AHM has been extended to solve various inverse problems such as (i) interpretation of relative permeability from laboratory core flooding data, (ii) estimation of permeability and skin factor of multilayered reservoir from injection-falloff test and (iii) characterization of hydraulic fractures in shale reservoirs from seismic and/or production data [18–20]. These previous studies indicated that the AHM is capable of deriving reasonable results with the proper experimental design and the implementation of robust algorithms. To date, various algorithms have been integrated with numerical simulation to assist history matching. Commonly used algorithms can be classified into two types. The first type is referred to as evolutionary optimization algorithms, such as the particle swarm optimization (PSO), genetic algorithm (GA), harmony search optimization (HSO), etc. The second type is referred to as the ensemble method, such as the ensemble Kalman filter (EnKF) and ensemble smoother with multiple data assimilation (ES-MDA). These algorithms have been reported to be capable of estimating the reservoir properties based on production data; however, hundreds or even thousands of numerical simulation runs are usually needed in order to obtain reasonable results [21,22]. Since numerical simulation runs regarding real well models are usually quite time-consuming, the AHM method involving these algorithms shares a common drawback of low efficiency.

To the best knowledge of the authors, the AHM method has not yet been applied for estimating the CBM reservoir properties based on well production data. This paper proposed the use of a newly developed high-efficiency algorithm, namely the Bayesian adaptive direct search (BADS) [23], to assist matching fractured vertical CBM well production in order to derive the reservoir properties. The applicability of the proposed method was tested on real CBM wells, and the superiority over typical existing algorithms was demonstrated.

2. Methods

2.1. Basics of the AHM

The AHM generally requires three components, namely a numerical or analytical simulator to simulate production behavior, an error function describing the mismatch between the simulated and real observed data and a specific algorithm to minimize the error function in order to obtain a "successful" matching.

In this study, all simulation runs were conducted using the numerical simulator GEM developed by the Computer Modelling Group [24]. The GEM is a compositional simulator that is capable of modeling CBM transport behavior including adsorption/desorption, gas diffusion, multi-phase seepage and stress- and sorption-induced permeability dynamics. The GEM simulator has been widely used to model fluid production behavior [25,26], to optimize well placement [27] and to evaluate the enhanced CBM potential [28] in CBM reservoirs.

The error function to be minimized was defined as the sum of the normalized squared errors between the simulated and observed data. The error function is written as:

$$E = \frac{\sum_{i=1}^{N}\left(y_i^{obs,g} - y_i^{sim,g}\right)^2}{\sum_{i=1}^{N}\left(y_i^{obs,g} - y^{avg,g}\right)^2} + \frac{\sum_{i=1}^{N}\left(y_i^{obs,w} - y_i^{sim,w}\right)^2}{\sum_{i=1}^{N}\left(y_i^{obs,w} - y^{avg,w}\right)^2} \quad (1)$$

where y is the variable to be matched; the superscripts "*obs*" and "*sim*" denote the observed and simulated data, respectively; superscripts "*g*" and "*w*" denote the gas and water, respectively; the superscript "*avg*" denotes the averaged value of the observed data; N is the total number of data points.

As stated previously, although a wide range of algorithms have been proposed to assist history matching, their efficiencies are questionable because a number of time-consuming simulation runs are needed before reasonable results can be obtained. Thus, this study proposed the usage of the BADS algorithm to accelerate the history matching process.

2.2. BADS Algorithm

The BADS algorithm is a fast, hybrid Bayesian optimization algorithm designed to solve difficult optimization problems, in particular related to fitting computational models. The BADS algorithm was first proposed by [23], which was then introduced by Zhang et al. [29] to be used for estimating relative permeability of coal based on laboratory flooding test data. The BADS is a hybridization of the Bayesian optimization (BO) [30] and mesh adaptive direct search (MADS) [31] algorithms. The mathematical details of the BADS are available in references [23,29]. For the completeness of this paper, the basics of the BADS are briefly introduced as follows.

Given a D_n-dimension minimization problem, BADS iteratively updates the solution variable vector (x) in a similar manner to MADS. In other words, BADS iteratively generates and evaluates the candidate solutions in two separate steps, namely the search and poll stages. In the search stage of the kth iteration, BADS generates candidate solutions by performing local optimization of the acquisition function in the neighborhood of the incumbent x_k. Commonly used acquisition functions include the lower confidence bound (LCB), upper confidence bound (UCB) and expected improvement (EI). In this study, we used the LCB acquisition function. The polling directions D_k are then constructed by scaling to the Gaussian process (GP) kernel length scales. In the polling stage, the solution candidates $\mathbf{x}_{\text{poll}}$ can be updated according to the following equation

$$x_{poll} = \{x_k + \Delta_k^m v : v \in D_k\} \quad (2)$$

where Δ_k^m is the mesh size at the kth iteration.

If the poll succeeds in sufficiently improving the objective function within three consecutive steps, the incumbent is updated, and BADS switches to a new iteration with mesh and poll sizes multiplied by $\tau = 2$; otherwise, the incumbent remains unchanged, and BADS switches to a new iteration with the mesh and poll sizes divided by $\tau = 2$. These steps are repeated until a preset maximum number of iterations is met, the algorithm stalls or the poll size becomes extremely small. During the iteration process, the accuracy of the surrogate models based on the GP is updated every $2D_n$ to $5D_n$ function evaluations and whenever the accuracy of the current GP is unreliable by refitting the hyperparameters of GP.

2.3. Setup of Reservoir Model

Proper setup of the reservoir model is the first important step to ensure the success of history matching. For the primary depletion of CBM reservoirs where no injector is involved, the single-well history matching is considered to be comparable with multi-well history matching in terms of matching accuracy provided that flowing boundary of each single well is properly defined [6]. Also, a lower number of wells indicates a lower number of parameters and reduced uncertainties, which can accelerate the convergence speed and reduce the risk of being trapped in local optima during history matching. Moreover, the single-well reservoir model has a far less number of grid blocks than multi-well models does and thus runs significantly faster. Therefore, this paper is primarily concerned with the single-well history matching process.

2.3.1. Construction of the Grid Model

Two types of well patterns are commonly used in CBM reservoirs, namely the five-spot (or diamond) and rectangular patterns [27]. For either well pattern, a single-well can be considered to be located in the center of its controlled area that is defined by the flowing boundaries. In this study, 3D uniform Cartesian grid models were constructed for the well to be history matched (Figure 1). Low-permeability coalbeds generally require relatively small well spacings in order to accelerate reservoir pressure drawdown and thus improve gas production [9,32,33]. For example, CBM wells are generally deployed at spacings in the range of 200~300 m in low-permeability CBM reservoirs in the Eastern Ordos and Southern Qinshui basins, China [34]. Zhang et al.'s optimization studies on well placement showed that the optimal well spacing for coalbeds with permeability less than 1.3 mD is approximately 250 m [27]. Considering the well spacing for low-permeability coalbeds, the number of grid blocks was set to be 61 both along the x- and y-direction. The x- and y-directions represent the face-cleat and butt-cleat directions, respectively. The dimension of each grid block was calculated to be the real well spacing divided by 61 along the x- and y-directions, respectively. For single-layered CBM reservoirs, the number of grid blocks in the vertical direction is set be unity. For multi-layered CBM reservoirs, the number of grid blocks in the vertical direction is set be the total number of coal seam layers and impermeable interlayers.

For each grid model, the grid blocks are divided into two regions. The first region represents the coalbed at the in situ condition that is not affected by hydraulic fracturing stimulation. The second region represents the hydraulic stimulated area (SA) around the well. The SA is simplified to be a rectangular area with the length and width in the face-and butt-cleat directions, respectively.

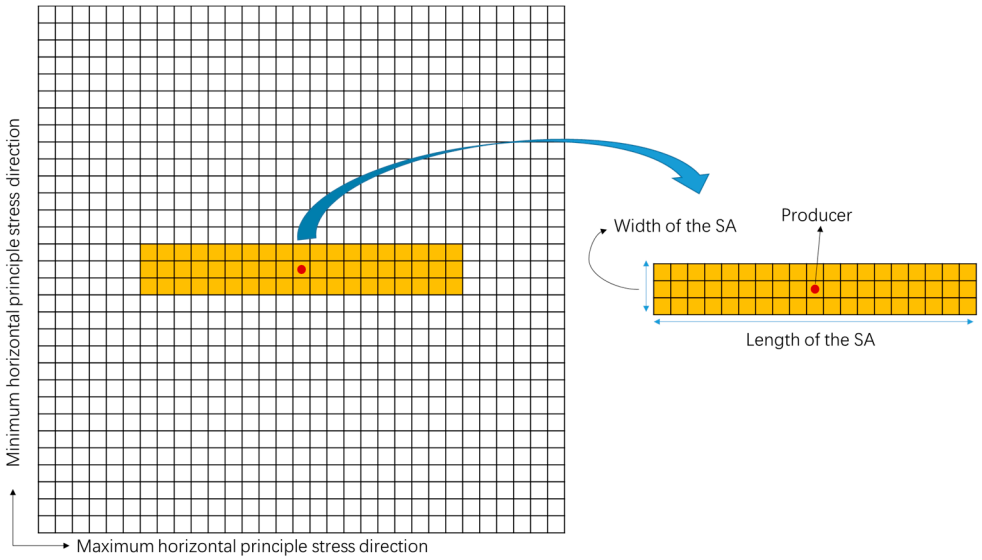

Figure 1. Illustration of the grid model.

2.3.2. Parameters to Be Tuned

Previous studies [12,15] have concluded that key parameters influencing gas and water productions in CBM reservoirs include coal seam thickness, sorption isotherm, porosity, permeability and relative permeability. For a real CBM well, the values of coal thickness, initial pressure and critical desorption pressure can be estimated with well logging and production data information. The sorption isothermal for a specific coalbed can be measured on cored samples in laboratory, which is a known parameter for the well where sample was cored. However, the sorption isothermal may vary from well to well due to differences in stress condition, water content, etc. Therefore, the sorption isothermal was also set to be tunable by adjusting the Langmuir volume and pressure within the common knowledge of the target coalbed. Porosity, permeability, permeability evolution dynamics and relative permeability are parameters associated with strong heterogeneities, which need to be tuned during history matching [11]. The permeability evolution dynamics were represented with the Palmer–Mansoori (PM) model [35], with the compressibility and sorption strain being the tunable parameters; other parameters in the PM model such as Poisson ratio, Young's Modulus and Langmuir pressure were fixed because these parameters are generally less uncertain for a given formation. The relative permeability was represented with a Corey-type model developed by Chen et al. [36] (Equation (3)). The relative permeability is varied by tuning the coefficients including the connate water saturation, endpoint water relative permeability and the exponents for the gas and water curves.

$$k_{rw} = k_{rw0} S_{wn}^{\lambda} \tag{3}$$

$$k_{rg} = (1 - S_{wn})^{\beta} \left(1 - S_{wn}^{\eta}\right) \tag{4}$$

$$S_{wn} = \frac{S_w - S_{wc}}{1 - S_{wc}} \tag{5}$$

where S_{wc} and S_{wn} are the connate and normalized water saturations, respectively; S_w is water saturation; k_{rw} and k_{rg} are relative permeability for the water and gas phases, respectively; k_{rw0} is the endpoint water relative permeability; λ, β and η are exponential coefficients that control the relative permeability curvature.

The hydraulic stimulation results in enhancement in flow capacity, which is represented by multiplying the permeability in the stimulated region by a factor in the range of one thousand to ten thousand [37]. Moreover, the embedment of proppants within

stimulated zones aids the retention of the fracture aperture [38]. Therefore, the coal deformation behavior and the consequent permeability dynamics due to reservoir pressure drawdown in the stimulated zones should be different from that in the un-stimulated zones. In this regard, two respective compressibility values were assigned in the stimulated and un-stimulated zones in order to model different deformation behaviors.

As a short summary, a total number of 16 properties need to be tuned during the history matching process, which include: (1) the length and width of the stimulated area; (2) two respective permeability values in the stimulated and un-stimulated zones; (3) two respective compressibility values in the stimulated and un-stimulated zones; (4) two respective sorption strain values in the stimulated and un-stimulated zones; (5) porosity; (6) sorption isotherm represented with Langmuir volume and Langmuir pressure; (7) relative permeability represented with five characteristic coefficients shown in Equations (3)–(5), namely S_{wc}, k_{rw0}, λ, β and η.

2.4. Workflow of the AHM

The workflow of AHM in this study includes the following 5 steps.

(1) Initializing the candidate solution vector x_0 subject to boundary constraints of physical meanings. For the BADS algorithm, the candidate solution is normalized within the range of [0, 1]. The normalized vector x is transformed into the real space X according to the following equation.

$$X = X_{lb} + (X_{ub} - X_{lb}) \cdot x \quad (6)$$

where the subscripts "ub" and "lb" denote the upper and lower boundaries of the parameter in the real space.

(2) Update the reservoir grid model data file and call the numerical simulator to run the model. The well is simulated under the bottom-hole pressure constraint to derive gas and water production.

(3) Calculate the matching error between the simulated and observed production data using Equation (1).

(4) Update the solution candidate with BADS based on the candidate solution and the corresponding error value at the previous iteration.

(5) Check the number of elapsed iterations. If the number of elapsed iterations does not reach the preset tolerance of the number of iterations, go back to step 2; otherwise, cease simulation and output the optimal solution that minimizes the matching error.

3. Case Study

The proposed method was applied on a number of representative CBM wells producing in the southern Qinshui Basin in order to demonstrate its applicability. The coals in the study area are anthracite in rank, which is characterized with low porosity, low permeability and high gas content. The coal formation is considered to be initially saturated with water. The selected wells were produced from the 3# coal seam of the Shanxi Formation. Wells were placed at an average spacing of 250 m, both in the face- and butt-cleat directions. All wells were hydraulically stimulated with silkwater following similar stimulation parameters, e.g., pumping rate, total injected fracturing fluid and sand ratio.

A number of three representative wells (referred to as Well #1, #2 and #3) were selected that are typical in terms of the gas production pattern. These wells are distributed within a distance of 2 km in the same block. Well #1 showed the highest gas producibility among the selected wells, with the maximum and average daily gas rates of 5730 and 1800 m^3/d, respectively. The daily gas rates of this well exhibit the "typical" trend of a CBM well: the gas rates first climbed and then declined sharply with the production duration. The gas production curve of Well #2 also exhibits a first increasing and then a decreasing trend. However, the decline in gas productions was sharp within the initial 500 days and then became gentle after the gas rate dropped to approximately below 1500 m^3/d. The peak and average gas rates were approximately 3000 and 1206 m^3/d, respectively, which were obviously lower than that of Well #1. Compared with the aforementioned two wells, Well

#3 showed a distinctive gas production pattern: the well had been producing at a relatively steady gas rate and did not show a sharp declining trend. The peak and average gas rates of Well #3 were 3000 and 1240 m^3/d, respectively. Wells were not considered that had experienced frequent workovers and showed severe fluctuations in production rates because these wells are associated with more uncertainties such as formation damage.

Since BADS is a stochastic algorithm in nature, uncertainties exist inevitably during the iteration process, and thus the ultimate optimal solution may vary from run to run. Therefore, the AHM was run five times for each well to evaluate the uncertainties associated with the optimal solutions. For each independent run, the searching point was randomly initialized, and the maximum number of function evaluations was set to be 120. Variables that have been addressed to exert minor effects on productions of initially water-saturated CBM reservoirs were set to be fixed, including the sorption time (10 days) and fracture spacing (0.5 cm). The well radius was set to be 0.06m according to the well completion report. For each AHM run, the upper and lower boundaries for variables to be estimated are given in Table 1. The boundary conditions of the sorption isothermals were set according to laboratory tests, which suggest coals in the target area generally have Langmuir volumes and pressures in the ranges of 24 to 40 m^3/t and 1.0 to 6.0 MPa, respectively. The boundary conditions for the in situ porosity, permeability and sorption strain were set empirically according to previous studies [11]. Coefficient ranges of the relative permeability model (Equation (3)) were adapted from Chen et al.'s summary on a number of relative permeability data [39]. The microseismic data monitored during the hydraulic fracturing process of CBM wells in the Qinshui basin suggest that the length of the SA is approximately 30 to 130 m, whereas the width of the SA is on the order of magnitude of tens of meters. In this study, the upper and lower boundaries were to be 50 to 100 for the length and 10 to 50 for the width of the SA. The permeability of the SA is associated with strong uncertainties and thus was varied in a relatively wide range of 1 to 50 mD. The compressibility and sorption strain were varied between 0.001 and 0.1 MPa^{-1} and between 0.005 and 0.03, respectively, in order to cover the ranges of anthracite coals according to laboratory tests.

Table 1. Boundary constraints of the variables to be estimated.

Variable	Lower Boundary	Upper Boundary
Porosity	0.001	0.05
In situ permeability, mD	0.01	1.0
In situ Compressibility, MPa^{-1}	0.001	0.1
Sorption strain	0.001	0.03
Langmuir volume, m^3/t	25	40
Langmuir pressure, MPa	1.0	6.0
S_{wc}	0	0.9
k_{rw0}	0.1	1
λ	0.1	10
β	0	5
η	1	10
Length of SA, m	50	120
Width of SA, m	10	50
Permeability of SA, mD	1	50
Compressibility of SA, MPa^{-1}	0.01	0.1

4. Results and Discussion

4.1. Performance of BADS

Figure 2 illustrates the objective function values during the iteration (minimization) process. As can be seen, the objective function decreases dramatically during the initial stage (within a number of 30 function evaluations) and then converges gradually to local optima. This suggests an alternation in mode from global exploration to local exploitation [29].

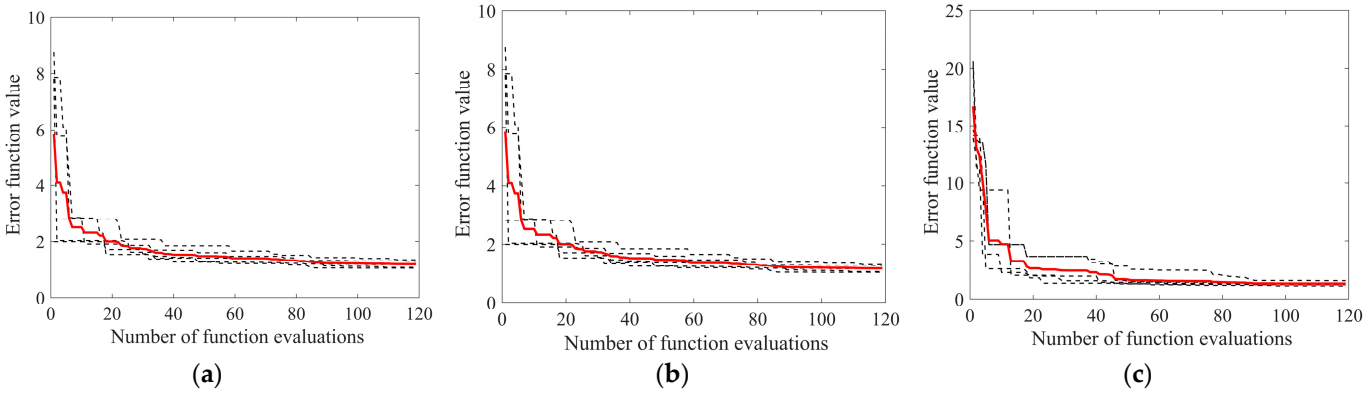

Figure 2. Evolution of the objective function value during the BADS searching process. (**a**) Well #1; (**b**) Well #2; (**c**) Well #3. The black dash lines represent five independent runs while the red solid lines are averaged values of the independent runs.

In the initial stage, BADS operated in a deterministic mode similar to the MADS algorithm, and thus the objection function values overlap with one another for the five independent runs. In the later stage (>30 iterations), BADS operated with stochasticity because the Bayesian process was involved; thus, different independent runs resulted in varied objection function values. However, very small differences were observed between different independent runs, suggesting strong robustness of BADS. It should also be noted that the number of function evaluations required for the BADS algorithm to achieve relatively stable convergence is noticeably small, which were approximately in the range of a number of 50 to 70 function evaluations. Since the numerical simulation run is usually time-consuming for a real model scenario, one may always anticipate less function evaluations in order to accelerate the AHM process. This highlights the high efficiency of the BADS algorithm in assisting achieving "successful" history matching results.

Figure 3 depicts the matching results with the minimized function values for the representative wells. As shown for each well, the independent AHM runs resulted in simulated production curves with slight deviations from one another possibly due to the stochastic nature of the BADS algorithm. Despite the distinct variation trends of the production data, the simulated production curves from all AHM runs agree well with the true ones for both gas and water phases. These observations suggested that the BADS is capable of deriving satisfactory matching results regardless of the production variation behaviors, which proved the adaptability of BADS for solving the AHM problems.

4.2. Comparison with Existing Algorithms

To demonstrate the superiority of BADS, the BADS algorithm was compared with two commonly used algorithms, namely particle swarm optimization (PSO) [40] and the covariance matrix adaptation evolution strategy (CMA-ES) [41] for history matching the aforementioned three wells. PSO and CMA-ES are stochastic algorithms with significant different underlying evolving mechanisms, which have been successfully applied for solving a variety of minimization problems including the AHM in the petroleum engineering community [42,43]. PSO and CMA-ES were independently applied for assisting the matching of the three wells. The maximum number of objective function evaluations was set to be 120, which was identical with that of the BADS. The hyperparameters of the PSO and CMA-ES were set to be default values as suggested by their original inventors. Each algorithm was independently run five times in order to evaluate their uncertainties.

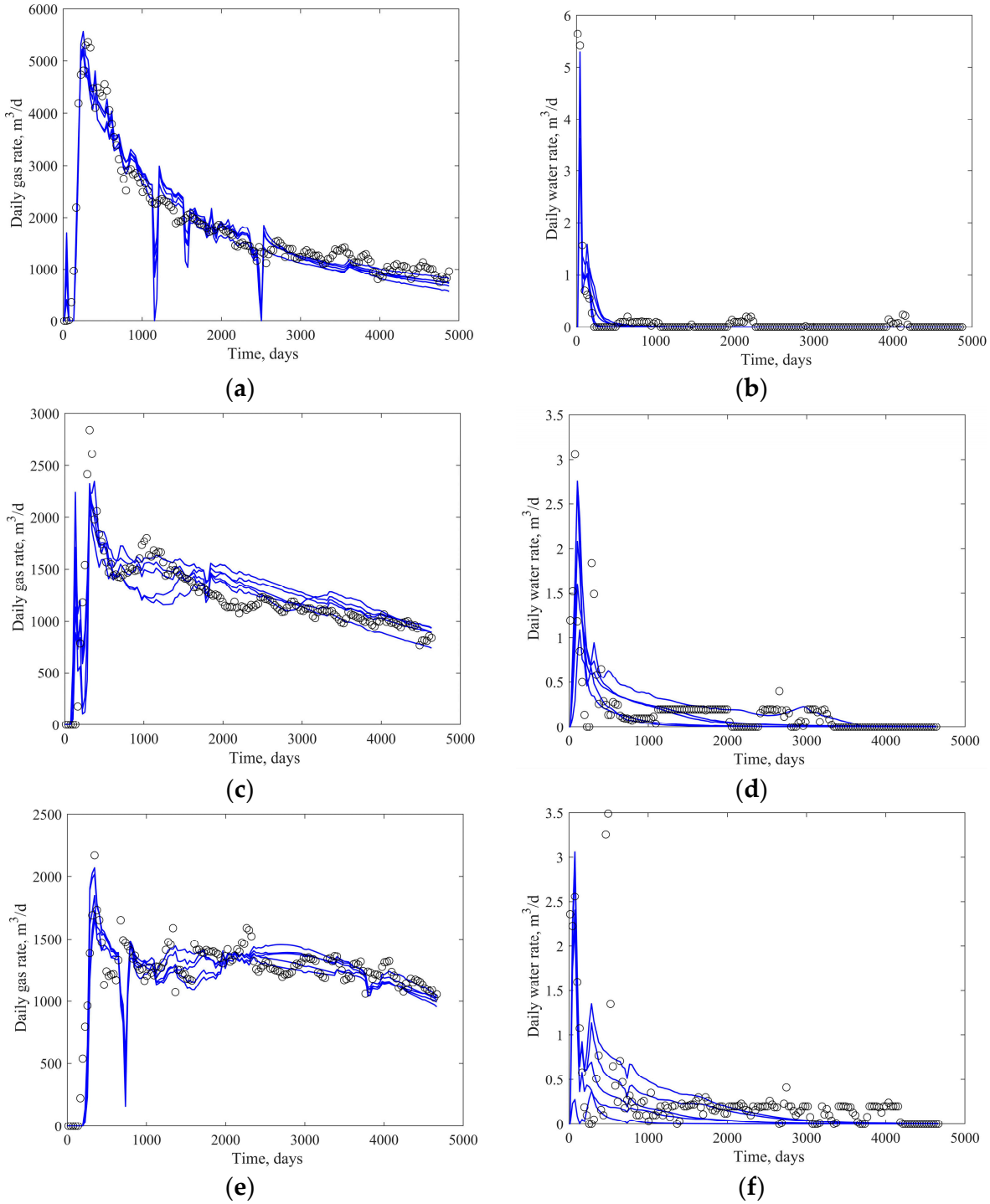

Figure 3. Comparison between the BADS-assisted simulated and true productions. (**a**,**c**,**e**) are gas productions of Well #1, #2 and #3, respectively; (**b**,**d**,**f**) are water productions of Well #1, #2 and #3, respectively. Open circles and blue lines represent the true and simulated productions, respectively.

Table 2 summarizes the minimized error function values with BADS, PSO and CMA-ES for the five independent runs, with the minimum, maximum and average values shown in Figure 4 for clear visualization. It can be seen from Table 2 and Figure 4 that BADS brought about smaller error function values to both the PSO and CMA-ES. The average minimized objective function values obtained from BADS were 0.657, 1.083 and 1.186 for Wells #1, #2 and #3, respectively. As a comparison, the CMA-ES resulted in obviously larger averaged error function values, which are 0.838, 1.636 and 1.996 for Wells #1, #2

and #3, respectively. The PSO performed better than the CMA-ES but worse than the BADS in terms of matching errors for all wells investigated. As shown in Figures 5 and 6, the resulting optimal solutions with PSO and the CMA-ES deviate severely from the true production data. The matrices and the visual figures suggest that BADS outperforms the remaining algorithms in terms of matching accuracy.

In addition to the average error, it is also important to evaluate the robustness of an algorithm considering the multiplicity nature of the history matching problems. In this study, we evaluated the robustness by comparing the deviations of the objective function values over five independent runs. As can be seen from Figure 4, very minor deviations exist with respect to the minimized errors over five independent runs with BADS. As a comparison, the minimized errors using PSO and CMA-ES are associated with obvious deviations over independent runs, especially for Wells #2 and #3 (Figure 4 and Table 2). The deviations of the minimized errors with the PSO and CMA-ES are approximately one order of magnitude of that with BADS. The large deviations among independent runs using the PSO and the CMA-ES are consistent with the resulting optimal solutions in Figures 5 and 6. As shown in Figures 5 and 6, the simulated production curves PSO and CMA-ES deviate severely from run to run, especially for Wells #2 and #3.

Table 2. Summary of the minimized objective function values using different algorithms.

Well ID	Algorithm	Minimized Objective Function Value							
		Run 1	**Run 2**	**Run 3**	**Run 4**	**Run 5**	**Max.**	**Min.**	**Avg.**
Well #1	BADS	0.729	0.626	0.644	0.661	0.624	0.729	0.624	0.657
	PSO	0.759	0.621	0.634	0.731	0.856	0.856	0.621	0.720
	CMA-ES	0.887	0.724	0.845	0.841	0.891	0.891	0.724	0.838
Well #2	BADS	1.081	1.132	1.038	1.140	1.022	1.140	1.022	1.083
	PSO	1.161	1.099	1.367	1.025	1.256	1.367	1.025	1.182
	CMA-ES	1.859	1.497	1.888	1.423	1.516	1.888	1.423	1.636
Well #3	BADS	1.102	1.041	1.128	1.396	1.265	1.396	1.041	1.186
	PSO	1.468	1.267	1.264	1.553	1.844	1.844	1.264	1.479
	CMA-ES	2.173	2.101	3.182	2.920	2.210	3.182	2.101	2.517

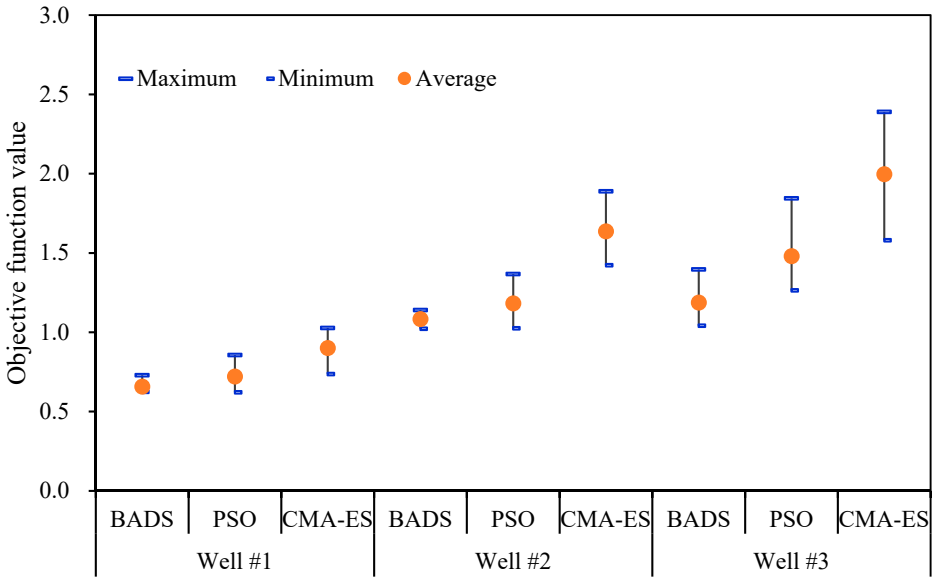

Figure 4. Comparison of BADS with PSO and CMA-ES.

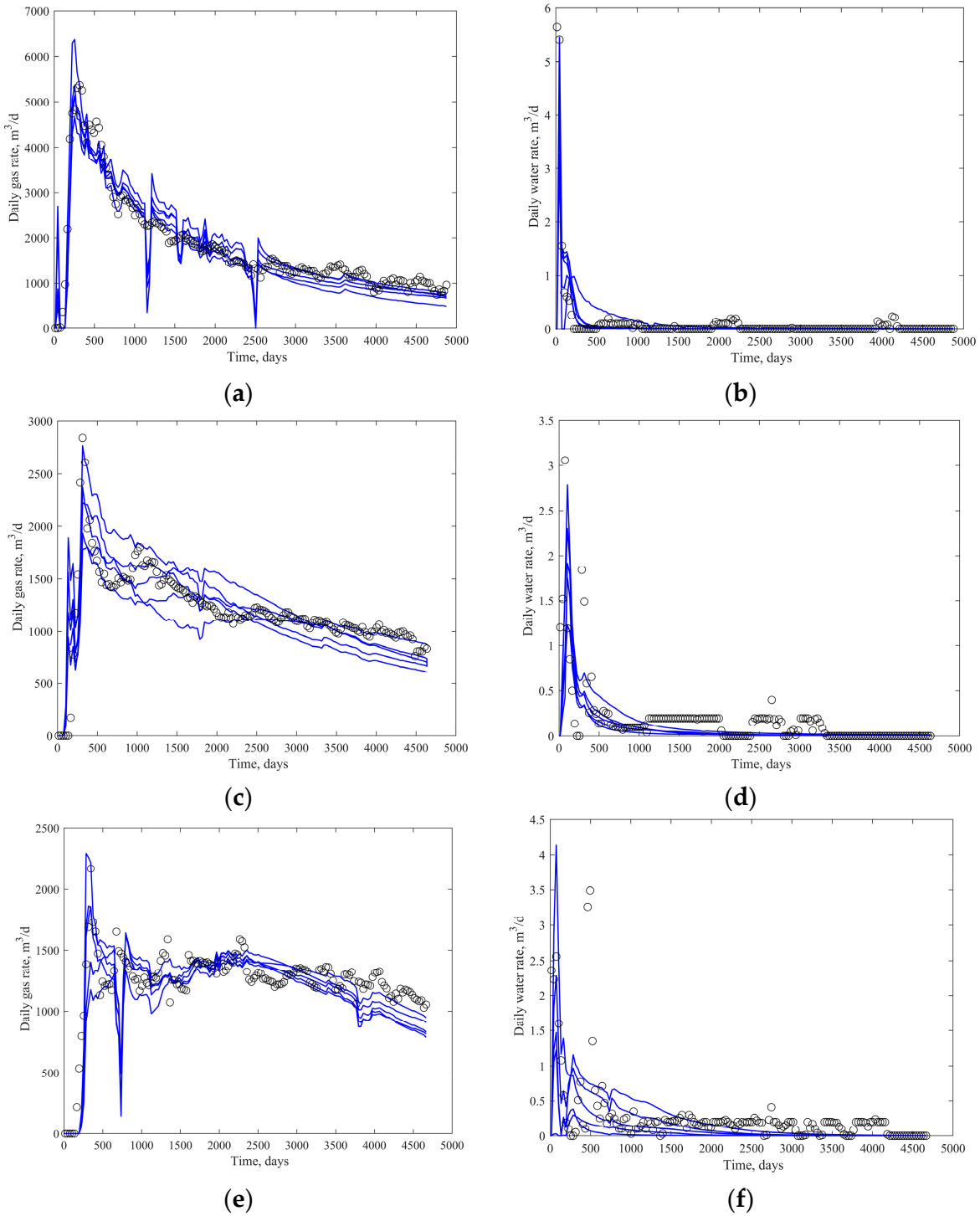

Figure 5. Comparison between the PSO-assisted simulated and true productions. (**a**,**c**,**e**) are gas productions of Well #1, #2 and #3, respectively; (**b**,**d**,**f**) are water productions of Well #1, #2 and #3, respectively. Open circles and blue lines represent the true and simulated productions, respectively.

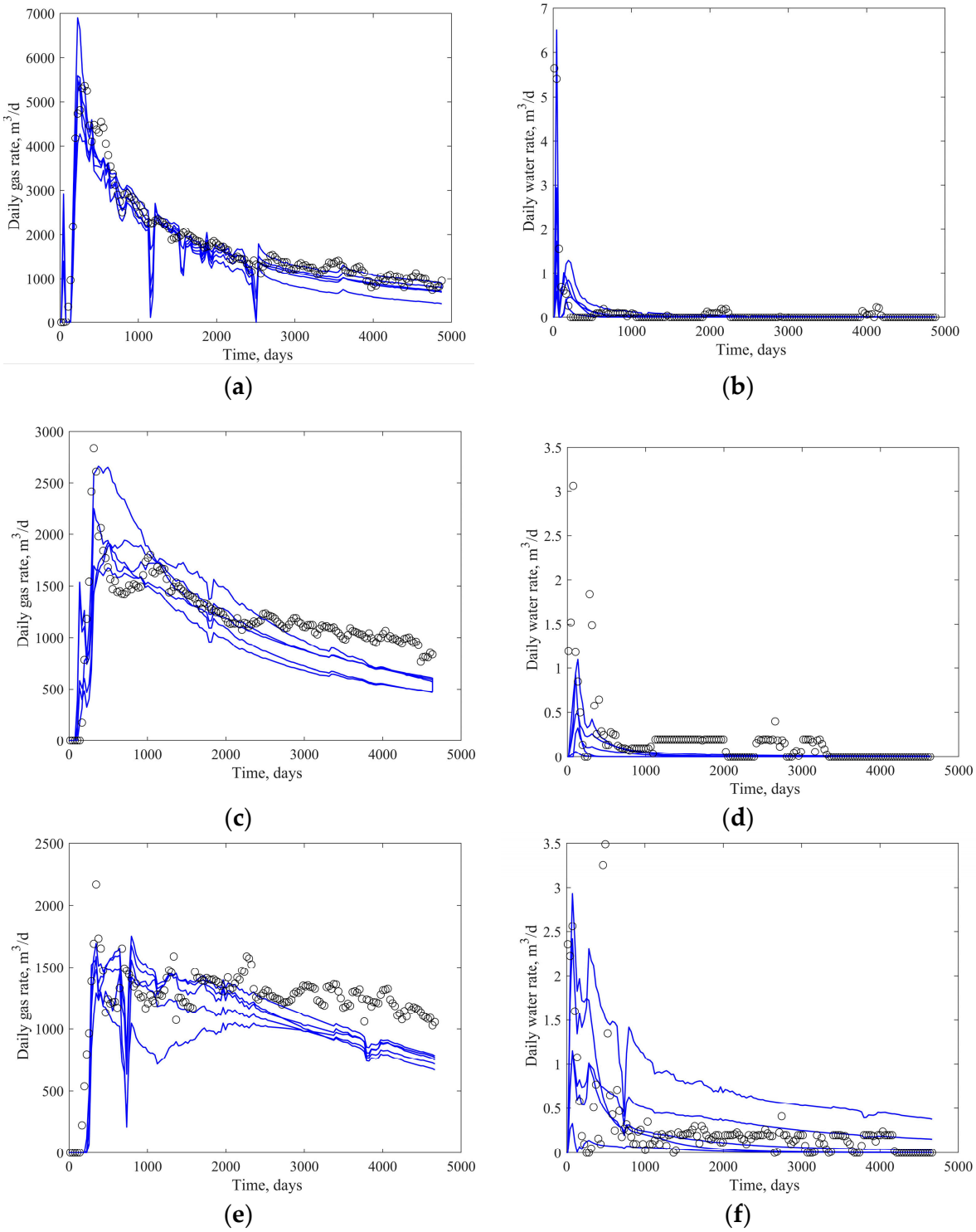

Figure 6. Comparison between the CMA-ES-assisted simulated and true productions. (**a**,**c**,**e**) are gas productions of Well #1, #2 and #3, respectively; (**b**,**d**,**f**) are water productions of Well #1, #2 and #3, respectively. Open circles and blue lines represent the true and simulated productions, respectively.

Figure 7 depicts the evolution trends of the error function values using PSO and CMA-ES as assisted algorithms. It can be seen that the error function values with the CMA-ES exhibit similar trend with the BADS; i.e., the error function drops dramatically within approximately a number of 50 function evaluations and then becomes relatively steady as more function evaluations are made. Nonetheless, CMA-ES results in remarkedly higher matching errors compared with BADS with a number of 120 function evaluations.

The error function values with the PSO exhibit similar trends with CMA-ES for Wells #1 and #3. However, the averaged error function values for Well #2 do not show an obvious convergence, which may indicate less efficiency of PSO.

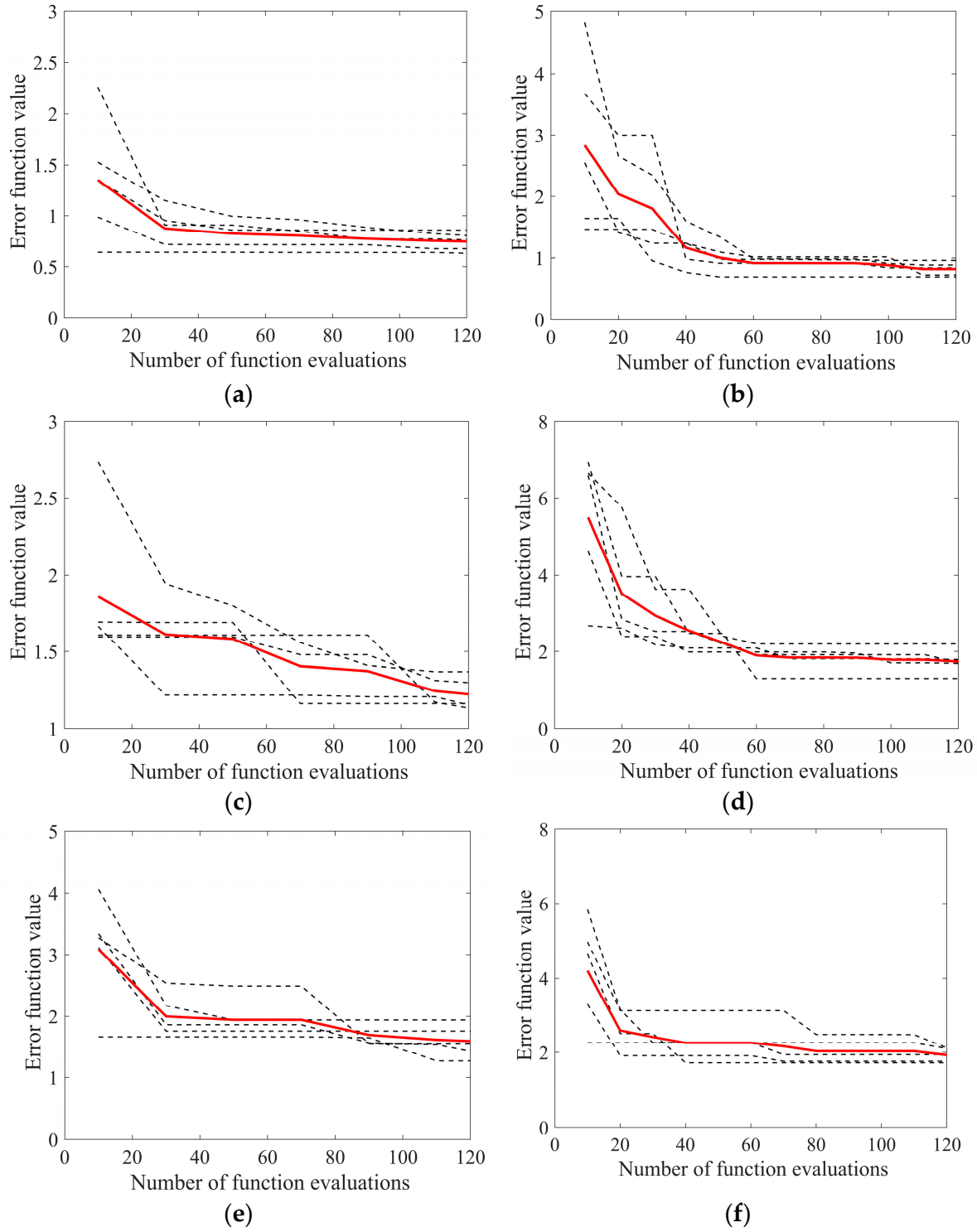

Figure 7. Evolution of the error function value during the AHM process using PSO and CAM-ES. (**a**,**c**,**e**) are using PSO for Well #1, #2 and #3, respectively; (**b**,**d**,**f**) are using CMA-ES for Well #1, #2 and #3, respectively. Dash lines represent the independent runs and red solid lines represent the averaged trend.

5. Conclusions

This paper proposed the use of the BADS algorithm to assist history matching of fractured vertical CBM wells. The proposed method was applied on CBM wells with representative production characteristics. The superiority of the BADS was highlighted by comparison with conventional algorithms including PSO and CMA-ES. Conclusions were summarized as follows.

(1) The BADS is capable of deriving reasonable results within a number of only 50–70 function evaluations, suggesting the high convergence speed and efficiency of BADS compared with existing methods. The resulting simulated gas and water productions agree well with true data.

(2) The performance of BADS in terms of matching accuracy was compared with two popular algorithms, namely PSO and CMA-ES. The resulting matching errors using BADS were significantly smaller than both the PSO and the CMA-ES algorithms. Moreover, BADS outperforms PSO and CMA-ES in terms of the robustness over repeated simulation runs.

Funding: This research was funded by PetroChina Huabei Oilfield Company, grant number HBYT-2022-JS-385.

Data Availability Statement: The data presented in this study are available on request from the corresponding author.

Acknowledgments: The author's thanks are owed to Jiyuan Zhang and Xiaodong Zhang from China University of Petroleum (East China) for their efforts in developing the code, assistance in translating the manuscript and fruitful discussions through the project.

Conflicts of Interest: The author declares no conflict of interest.

References

1. Díaz, M.B.; González, N.C. Control and prevention of gas out-bursts in coal mines, Riosa-Olloniego-coalfifield, Spain. *Int. J. Coal Geol.* **2007**, *69*, 235–266.
2. Zhang, J.; Xu, K.; Reniers, G.; You, G. Statistical analysis the characteristics of extraordinarily severe coal mine accidents (ESCMAs) in China from 1950 to 2018. *Process Saf. Environ.* **2020**, *133*, 332–340. [CrossRef]
3. Karacan, C.O.; Ruiz, F.A.; Cote, M.; Phipps, S. Coal mine methane: A review of capture and utilization practices with benefits to mining safety and to green-house gas reduction. *Int. J. Coal Geol.* **2011**, *86*, 121–156. [CrossRef]
4. Karimpouli, S.; Tahmasebi, P.; Ramandi, H.L. A review of experimental and numerical modeling of digital coalbed methane: Imaging, segmentation, fracture modeling and permeability prediction. *Int. J. Coal Geol.* **2020**, *228*, 103–552. [CrossRef]
5. Cong, H.R.; Wang, K.; Wang, G.D.; Yang, X.; Du, F. Underground coal seam gas displacement by injecting nitrogen: Field test and effect prediction. *Fuel* **2021**, *306*, 121–646.
6. Karacan, C.Ö. Single-well production history matching and geostatistical modeling as proxy to multi-well reservoir simulation for evaluating dynamic reservoir properties of coal seams. *Int. J. Coal Geol.* **2021**, *241*, 103–766. [CrossRef]
7. Xu, H.J.; Pan, Z.J.; Hu, B.L.; Liu, H.H.; Sun, G. A new approach to estimating coal gas content for deep core sample. *Fuel* **2020**, *277*, 118–246. [CrossRef]
8. Mavor, M.J.; Close, J.C.; McBane, R.A. Formation Evaluation of Exploration Coalbed Methane Wells. In Proceedings of the SPE/CIM International Technical Meeting, Calgary, AB, Canada, 10–13 June 1990.
9. Feng, Q.; Zhang, J.; Zhang, X.; Hu, A. Optimizing well placement in a coalbed methane reservoir using the particle swarm optimization algorithm. *Int. J. Coal Geol.* **2012**, *104*, 34–45. [CrossRef]
10. Zhou, F. History matching and production prediction of a horizontal coalbed methane well. *J. Petrol. Sci. Eng.* **2012**, *96–97*, 22–36. [CrossRef]
11. Zhang, J.; Feng, Q.; Zhang, X.; Hu, Q.; Wen, S.; Chen, D.; Zhai, Y.; Yan, X. Multi-fractured horizontal well for improved coalbed methane production in eastern Ordos basin, China: Field observations and numerical simulations. *J. Petrol. Sci. Eng.* **2020**, *194*, 107488. [CrossRef]
12. Akhondzadeh, H.; Keshavarz, A.; Sayyafzadeh, M.; Kalantariasl, A. Investigating the relative impact of key reservoir parameters on performance of coalbed methane reservoirs by an efficient statistical approach. *J. Nat. Gas. Sci. Eng.* **2018**, *53*, 416–428. [CrossRef]
13. Zuber, M.D.; Olszewski, A.J. The impact of errors in measurement of coalbed methane reservoir properties on well production forecasts. In Proceedings of the 62nd SPE Annual Technical Conference and Exhibition, Dallas, TX, USA, 27–30 September 1987.
14. Young, G.B.C.; Paul, G.W.; McElhiney, J.E. A parametric analysis of Fruitland Coalbed methane producibility. In Proceedings of the 67th SPE Annual Technical Conference and Exhibition, Washington, DC, USA, 4–7 October 1992.

15. Duan, L.J.; Zhou, F.D.; Xia, Z.H.; Qu, L.C.; Yi, J. New Integrated History Matching Approach for Vertical Coal Seam Gas Wells in the KN Field, Surat Basin, Australia. *Energy Fuels* **2020**, *34*, 15829–15842. [CrossRef]
16. Li, B.; Bhark, E.W.; Gross, S.J.; Billiter, T.C.; Dehghani, K. Best Practices of Assisted History Matching Using Design of Experiments. *SPE J.* **2019**, *24*, 1435–1451. [CrossRef]
17. Tripoppoom, S.; Xie, J.; Yong, R.; Wu, J.; Yu, W.; Sepehrnoori, K.; Miao, J.; Chang, C.; Li, N. Investigation of different production performances in shale gas wells using assisted history matching: Hydraulic fractures and reservoir characterization from production data. *Fuel* **2020**, *267*, 117–1097. [CrossRef]
18. Wu, H.Y.; Cheng, L.S.; Killough, J.; Huang, S.J.; Fang, S.D.; Jia, P.; Cao, R.; Xue, Y.C. Integrated characterization of the fracture network in fractured shale gas Reservoirs—Stochastic fracture modeling, simulation and assisted history matching. *J. Petrol. Sci. Eng.* **2021**, *205*, 108–886. [CrossRef]
19. Nejadi, S.; Leung, J.Y.; Trivedi, J.J.; Claudio, V. Integrated Characterization of Hydraulically Fractured Shale-Gas Reservoirs—Production History Matching. *SPE Res. Eval. Eng.* **2015**, *18*, 481–494. [CrossRef]
20. Shams, M.; El-Banbi, A.; Sayyouh, H. Harmony search optimization applied to reservoir engineering assisted history matching. *Petrol. Explor. Dev.* **2020**, *47*, 154–160. [CrossRef]
21. Zhang, Y.; Song, C.; Yang, D. A damped iterative EnKF method to estimate relative permeability and capillary pressure for tight formations from displacement experiments. *Fuel* **2016**, *167*, 306–315. [CrossRef]
22. Zhang, Y.; Fan, Z.Q.; Yang, D.Y.; Li, H.; Shirish, P. Simultaneous Estimation of Relative Permeability and Capillary Pressure for PUNQ-S3 Model With a Damped Iterative-Ensemble-Kalman-Filter Technique. *SPE J.* **2000**, *22*, 971–984. [CrossRef]
23. Acerbi, L.; Ma, W.J. Practical Bayesian Optimization for Model Fitting with Bayesian Adaptive Direct Search. *Adv. Neural Inform. Process. Syst.* **2017**, *30*, 1834–1844.
24. Computer Modelling Group. *User Guide: Compositional & Unconventional Reservoir Simulator*; Computer Modelling Group: Calgary, AB, Canada, 2015.
25. Ziarani, A.S.; Aguilera, R.; Clarkson, C.R. Investigating the effect of sorption time on coalbed methane recovery through numerical simulation. *Fuel* **2011**, *90*, 2428–2444. [CrossRef]
26. Karacan, C.O.; Olea, R.A. Stochastic reservoir simulation for the modeling of uncertainty in coal seam degasification. *Fuel* **2015**, *148*, 87–97. [CrossRef]
27. Zhang, J.; Feng, Q.; Zhang, X.; Bai, J.; Karacan, C.Ö.; Wang, Y.; Elsworth, D. A two-stage step-wise framework for fast optimization of well placement in coalbed methane reservoirs. *Int. J. Coal Geol.* **2020**, *225*, 103479. [CrossRef]
28. Mohammadpoor, M.; Firouz, A.Q.; Torabi, F. Implementing Simulation and Artificial Intelligence Tools to Optimize the Performance of the CO_2 Sequestration in Coalbed Methane Reservoirs. In Proceedings of the Carbon Management Technology Conference, Orlando, FL, USA, 7–9 February 2012.
29. Zhang, J.; Zhang, B.; Xu, S.; Feng, Q.; Zhang, X.; Elsworth, D. Interpretation of Gas/Water Relative Permeability of Coal Using the Hybrid Bayesian-Assisted History Matching: New Insights. *Energies* **2021**, *14*, 626. [CrossRef]
30. Snoek, J.; Larochelle, H.; Adams, R.P. Practical Bayesian optimization of machine learning algorithms. In Proceedings of the Advances in Neural Information Processing Systems, Lake Tahoe, NV, USA, 3–6 December 2012; pp. 2951–2959.
31. Audet, C.; Dennis, J.E. Mesh adaptive direct search algorithms for constrained optimization. *SIAM J. Optimiz.* **2006**, *17*, 188–217. [CrossRef]
32. Zuber, M.D.; Kuuskraa, V.A.; Walter, K.S. Optimizing Well Spacing and Hydraulic-Fracture Design for Economic Recovery of Coalbed Methane. *SPE Form Eval.* **1990**, *5*, 98–102. [CrossRef]
33. Maricic, N.; Mohaghegh, S.D.; Artun, E. A Parametric Study on the Benefits of Drilling Horizontal and Multilateral Wells in Coalbed Methane Reservoirs. *SPE Res. Eval. Eng.* **2008**, *11*, 976–983. [CrossRef]
34. Meng, Z.; Zhang, K.; Yang, J.; Lei, J.; Wang, Y. Analysis of coal reservoir characteristics in the Qin-nan-East block and its spacing optimization of CBM development well networks. *J. China Coal Soc.* **2018**, *43*, 2525–2533, (In Chinese with English abstract).
35. Ian, P.; Mansoori, J. How Permeability Depends on Stress and Pore Pressure in Coalbeds: A New Model. *SPE Res. Eval. Eng.* **1998**, *1*, 539–544.
36. Chen, D.; Pan, Z.; Liu, J.; Connell, L.D. An improved relative permeability model for coal reservoirs. *Int. J. Coal Geol.* **2013**, *109*, 45–57. [CrossRef]
37. King, G.R.; Ertekin, T. Comparative evaluation of vertical and horizontal drainage wells for the degasification of coal seams. *SPE Reserv. Eng.* **1988**, *3*, 720–734. [CrossRef]
38. Kumar, H.; Elsworth, D.; Liu, J.; Pone, D.; Mathews, J.P. Permeability evolution of propped artificial fractures in coal on injection of CO_2. *J. Petrol. Sci. Eng.* **2015**, *133*, 695–704. [CrossRef]
39. Chen, D.; Shi, J.Q.; Durucan, S.; Korre, A. Gas and water relative permeability in different coals: Model match and new insights. *Int. J. Coal Geol.* **2014**, *122*, 37–49. [CrossRef]
40. Kennedy, J. Particle swarm optimization. In Proceedings of the 1995 IEEE International Conference on Neural Networks, Perth, WA, Australia, 27 November–1 December 1995; Volume 4, pp. 1942–1948.
41. Hansen, N.; Ros, R.; Mauny, N.; Schoenauer, M.; Auger, A. Impacts of invariance in search: When CMA-ES and PSO face ill-conditioned and non-separable problems. *APPL Soft. Comput.* **2011**, *11*, 5755–5769. [CrossRef]

42. Xiang, W.; Haynes, R.D.; Feng, Q. A multilevel coordinate search algorithm for well placement, control and joint optimization. *Comput. Chem. Eng.* **2016**, *95*, 75–96.
43. Mohamed, L.; Christie, M.; Vasily, D. Comparison of Stochastic Sampling Algorithms for Uncertainty Quantification. *SPE J.* **2010**, *15*, 31–38. [CrossRef]